



Universiteit  
Leiden  
The Netherlands

## **Spin-label EPR on Disordered and Amyloid Proteins**

Hashemi Shabestari, M.

### **Citation**

Hashemi Shabestari, M. (2013, April 16). *Spin-label EPR on Disordered and Amyloid Proteins*. Retrieved from <https://hdl.handle.net/1887/20749>

Version: Not Applicable (or Unknown)

License: [Leiden University Non-exclusive license](#)

Downloaded from: <https://hdl.handle.net/1887/20749>

**Note:** To cite this publication please use the final published version (if applicable).

Cover Page



Universiteit Leiden



The handle <http://hdl.handle.net/1887/20749> holds various files of this Leiden University dissertation.

**Author:** Hashemi Shabestari, Maryam

**Title:** Spin-label EPR on disordered and amyloid proteins

**Issue Date:** 2013-04-16

## **CHAPTER 4**

### **THE AGGREGATION POTENTIAL OF 1-15 AND 1-16 FRAGMENTS OF THE AMYLOID $\beta$ PEPTIDE AND THEIR INFLUENCE ON THE AGGREGATION OF A $\beta$ 40**

The aggregation of amyloid  $\beta$  (A $\beta$ ) peptide is important in Alzheimer's disease. Shorter A $\beta$  fragments may reduce A $\beta$ 's cytotoxicity and are used in diagnostics. The aggregation of A $\beta$ 16 is controversial; Liu et al. (*J. Neurosci. Res.* **2004**, 72, 162-171) and Liao et al. (*FEBS Lett.* **2007**, 581, 1161-1165) find that A $\beta$ 16 does not aggregate and reduces A $\beta$ 's cytotoxicity, Du et al. (*J. Alzheimers Dis.* **2011**, 27, 401-413) reports that A $\beta$ 16 aggregates and that A $\beta$ 16 oligomers are toxic to cells. Here the aggregation potential of two shorter fragments, A $\beta$ 15 and A $\beta$ 16, and their influence on A $\beta$ 40 is measured by Electron Paramagnetic Resonance (EPR) spectroscopy and the Thioflavin T fluorescence assay (ThioT). Continuous wave, 9 GHz EPR measurements and ThioT results reveal that neither A $\beta$ 15 nor A $\beta$ 16 aggregate by themselves and that they do not affect A $\beta$ 40 aggregation.

M. Hashemi Shabestari, T. Plug, M.M. Motazacker, N.J. Meeuwenoord, D.V. Filippov, J.C.M. Meijers, M. Huber.

## 4.1 Introduction

Fibrillar plaques and aggregates of the 39 to 42 amino-acid residue amyloid  $\beta$  ( $A\beta$ ) peptide in the brain have been recognized as major characteristics of Alzheimer's disease <sup>[1-4]</sup>. The  $A\beta$  peptide originates from a proteolytic cleavage of the amyloid precursor protein (APP), a human transmembrane protein crucial for memory <sup>[3,5]</sup>. Recently, more than about 20 shorter  $A\beta$  fragments, comprising residues 1-15, 4-15, 5-15, 14-15, 1-13, 1-14, etc. of the N-terminus of the full-length  $A\beta$  (table 4.1), have been reported in the cerebrospinal fluid (CSF), in addition to the previously reported  $A\beta$ 1-16 fragment ( $A\beta$ 16) <sup>[6-9]</sup>. Some of these fragments are up-regulated in Alzheimer's disease <sup>[6,7]</sup>. The soluble  $A\beta$ 16 fragment in the brain results from the cleavage between amino acids  $K_{16}$  and  $L_{17}$ , the proposed  $\alpha$ -secretase cleavage site in the  $A\beta$  sequence. Amongst the 20  $A\beta$  fragments that are upregulated, 11 fragments with different length end at amino acid 15, one amino acid before the  $\alpha$ -secretase cleavage site, which suggests a novel metabolic pathway for APP <sup>[6,7]</sup>. The short  $A\beta$  fragments draw a lot of attention especially in the search for peptide or peptidomimetic inhibitors of  $A\beta$  aggregation in the pathological context <sup>[8,10,11]</sup>. For example the  $A\beta$ 1-15 fragment ( $A\beta$ 15) can be used as a vaccine <sup>[12,13]</sup>. However, the precise sequence of events through which these short fragments form and their role in aggregation and toxicity of the full-length  $A\beta$  are still under debate. Reports about the aggregation potential of the N-terminal  $A\beta$  fragments by themselves are discrepant. According to Liu et al. <sup>[14]</sup> and Liao et al. <sup>[15]</sup>,  $A\beta$ 16 does not aggregate and reduces  $A\beta$ 's cytotoxicity in neuronal cells, whereas Du et al. <sup>[16]</sup> report that  $A\beta$ 16 aggregates and that  $A\beta$ 16 oligomers are toxic to cells. Du et al. <sup>[16]</sup> also show that  $A\beta$ 15 forms aggregates, which are not toxic to cells. These conflicting results, obtained by NMR <sup>[17-19]</sup>, FTIR, AFM, and CD <sup>[14-16]</sup> prompted us to investigate the behavior of these N-terminal  $A\beta$  fragments by a different technique. We used spin-label EPR and ThioflavinT fluorescence assay to study the fragments  $A\beta$ 15 and  $A\beta$ 16 (for sequence see table 4.1). Earlier, it was shown that signatures of the oligomeric  $A\beta$  peptide can be detected by the spin-label EPR methodology, which suggests this technique as a possible tool to detect the early stages of aggregation of the  $A\beta$  peptide <sup>[20]</sup>. Here we employ spin-label EPR to investigate and compare the aggregation potential of  $A\beta$ 15 and of  $A\beta$ 16, and their influence on the aggregation of  $A\beta$ 40. We combined spin-label EPR with diamagnetic dilution, in which the spin-labeled  $A\beta$  peptide (SL- $A\beta$ ) is diluted with unlabeled  $A\beta$  peptide (wild type  $A\beta$  peptide) to avoid line broadening by spin-spin interaction <sup>[20-22]</sup>.

**Table 4.1** The amino-acid sequence of the full-length A $\beta$  peptide (A $\beta$ 40) and the two fragments, A $\beta$ 15 and A $\beta$ 16 studied here. Residues 15 and 16 of A $\beta$  peptide are glutamine and lysine, respectively. The cysteine variants (Cys-A $\beta$ ) of each of the three peptides with an additional cysteine at the N-terminus are used for spin labeling.

A $\beta$ peptide	amino-acid sequence
Cys-A $\beta$ 15	CD <sub>1</sub> A <sub>2</sub> E <sub>3</sub> F <sub>4</sub> R <sub>5</sub> H <sub>6</sub> D <sub>7</sub> S <sub>8</sub> G <sub>9</sub> Y <sub>10</sub> E <sub>11</sub> V <sub>12</sub> H <sub>13</sub> H <sub>14</sub> Q <sub>15</sub>
Cys-A $\beta$ 16	CD <sub>1</sub> A <sub>2</sub> E <sub>3</sub> F <sub>4</sub> R <sub>5</sub> H <sub>6</sub> D <sub>7</sub> S <sub>8</sub> G <sub>9</sub> Y <sub>10</sub> E <sub>11</sub> V <sub>12</sub> H <sub>13</sub> H <sub>14</sub> Q <sub>15</sub> K <sub>16</sub>
Cys-A $\beta$ 40	CD <sub>1</sub> A <sub>2</sub> E <sub>3</sub> F <sub>4</sub> R <sub>5</sub> H <sub>6</sub> D <sub>7</sub> S <sub>8</sub> G <sub>9</sub> Y <sub>10</sub> E <sub>11</sub> V <sub>12</sub> H <sub>13</sub> H <sub>14</sub> Q <sub>15</sub> K <sub>16</sub> L <sub>17</sub> V <sub>18</sub> F <sub>19</sub> F <sub>20</sub> A <sub>21</sub> E <sub>22</sub> D <sub>23</sub> V <sub>24</sub> G <sub>25</sub> S <sub>26</sub> N <sub>27</sub> K <sub>28</sub> G <sub>29</sub> A <sub>30</sub> I <sub>31</sub> I <sub>32</sub> G <sub>33</sub> L <sub>34</sub> M <sub>35</sub> V <sub>36</sub> G <sub>37</sub> G <sub>38</sub> V <sub>39</sub> V <sub>40</sub>

By spin-label EPR, the mobility of the peptide is directly monitored enabling the detection of even small amounts (< 10 %) of aggregate, which would be difficult by the methods currently employed <sup>[23,24]</sup>. We demonstrate that under the conditions of our experiments neither A $\beta$ 15 nor A $\beta$ 16 aggregate and that they do not seem to affect full-length A $\beta$  aggregation.

## 4.2 Materials and methods

The A $\beta$ 40 peptide and its cysteine-A $\beta$  variant (H-Cys-Asp-Ala-...-Val-OH) were purchased from AnaSpec (purity > 95 %). The A $\beta$ 15 and A $\beta$ 16 and their cysteine-A $\beta$  variants were purchased from Peptide 2.0 Inc, Chantilly, VA (purity > 95 %), the solvent DMSO was purchased from Biosolve (purity 99.8 %). the MTS spin label ((1-oxyl-2,2,5,5-tetramethylpyrroline-3-methyl) methanethiosulfonate) was purchased from Toronto Research Chemicals Inc. (Brisbane Rd., North York, Ontario, Canada, M3J 2J8). Spin labeling was performed and the purified spin-labeled A $\beta$  was analyzed by liquid chromatography as described previously <sup>[20]</sup>. The peptides were lyophilized and stored in the freezer (-20° C) until used.

### 4.2.1 Sample preparation protocol

The A $\beta$  peptide samples in phosphate-buffered saline (PBS, 12 mM Na<sub>2</sub>HPO<sub>4</sub>, 137 mM NaCl, 2.7 mM KCl, 1.8 mM KH<sub>2</sub>PO<sub>4</sub> at pH 7.4) were prepared as diamagnetically diluted (dd) samples according to the protocol reported before <sup>[20]</sup>. Typical samples contained a mixture of 86 % wild type A $\beta$  and 14 % SL-A $\beta$ . Two peptide concentrations (0.55 mM and 1.1 mM) were investigated. For the shorter peptides, the spin-labeled shorter peptides were mixed either with the respective wild type peptide or with the wild type A $\beta$ 40. A typical sample of SL-A $\beta$ 15 with wild type A $\beta$ 40 had the following concentrations: 0.077 mM SL-A $\beta$ 15, 0.47 mM wild type A $\beta$ 15 (dd-SL-A $\beta$ 15) and 0.55 mM wild type A $\beta$ 40. To investigate the

effect of shorter peptides on the A $\beta$ 40 peptide, either of the wild type shorter peptides was added to the SL-A $\beta$ 40 sample.

### 4.2.2 EPR experiments

Samples of 10-15  $\mu$ l peptide solution were drawn into Blaubrand 50  $\mu$ l capillaries. The X-band continuous wave EPR measurements were performed using an ELEXSYS E680 spectrometer (Bruker, Rheinstetten, Germany) equipped with a rectangular cavity. A modulation frequency of 100 kHz was used for all measurements; the accumulation time for the spectra was 40 minutes per spectrum. Samples were measured at room temperature (20° C) using 6.331 mW microwave power and a modulation amplitude of 1.4 G. The large modulation amplitude ensured a better signal-to-noise ratio for broad lines. The measurements were made immediately after dissolving in PBS. Samples were kept at room temperature in these capillaries for 10 days without agitation and measured again after two, seven, and 10 days to monitor time dependent effects. In all cases, the spectra were identical to those measured initially (data not shown).

### 4.2.3 Simulations of EPR spectra

The spectra were simulated using Matlab and the EasySpin package <sup>[25]</sup>. For the simulation the following parameters were used:  $g = [2.00906, 2.00687, 2.00300]$  <sup>[20,26]</sup> and  $A_{xx} = A_{yy} = 12$  and 13 MHz in DMSO and buffer, respectively. Over-modulation effects were taken into account in EasySpin. According to the simulation, the EPR spectra were composed of three components of different mobilities. These components were referred to as fast, medium, and slow according to their rotation correlation times ( $\tau_r$ ) as reported before <sup>[20]</sup>.

### 4.2.4 Ratio of the intensity of the “fast” and “slow” components in each spectrum

Another way to define the mobility of the spin label, rather than by the relatively time-consuming simulations, is to measure amplitude ratios directly from the spectra <sup>[20,27,28]</sup>. Here we use the amplitude ratio of the mobile component to the strongly immobilized component. The contribution of these two components was obtained by selecting specific positions in the EPR spectra ( $B_{0slow} = 334.3 \pm 0.1$  mT;  $B_{0fast} = 337.3 \pm 0.1$  mT) at which one component has a large amplitude and the other a small one. The ratio of the fast to slow component, i.e., the ratio of the amplitudes of the two selected spectral positions (see results) gives an indication of the aggregation state of the peptide. The larger the ratio, the smaller is the degree of aggregation in the sample. The values and the sample to sample variation of this ratio (standard deviation) were determined for three independent sets of samples.

#### **4.2.5 Thioflavin T fluorescence assay**

As there is a stoichiometric and saturable interaction between ThioT and amyloid fibrils, fluorescence from the amyloid-ThioT complex provides accurate quantification of amyloid fibril formation as a function of amyloid fibril number [29,30]. For the ThioT fluorescence assay, six different A $\beta$  peptide samples, differing in A $\beta$  peptide content were investigated. For the full-length peptide two peptide concentrations (0.55 mM and 1.1 mM) and for the shorter peptides one concentration (0.55 mM) was investigated. To examine the effect of shorter peptides on the A $\beta$ 40 peptide, 1:1 mixtures of the shorter peptides with the full-length peptide (total peptide concentration of 1.1 mM) were prepared. For ThioT readings, the peptide was diluted with 10  $\mu$ M ThioT in 50 mM glycine/NaOH buffer, pH 8.6. The final concentration of peptide in the ThioT wells was 11  $\mu$ M or 27.5  $\mu$ M. Fluorescence was measured with the Fluostar Galaxy fluorometer, 96 well, Black, uClear–Plate Ref. 655090 Greiner (fluor plate). The settings were: excitation  $\lambda$ : 450 nm emission  $\lambda$ : 485 nm, 1 cycle, 10 flashes, and gain: 75. All samples were prepared and measured at least three times.

#### **4.3 Results**

Figure 4.1 shows the continuous-wave EPR spectra of SL-A $\beta$ 15 in DMSO and in PBS measured at room temperature. The spectrum of the SL-A $\beta$ 15 peptide under aggregation conditions (in PBS) is similar to the spectrum of the peptide in DMSO, a solvent in which amyloid peptides are in the monomeric form [31-33]. The same is true for the EPR spectra of SL-A $\beta$ 16 in PBS and in DMSO (spectra not shown), which indicates that A $\beta$ 15 and A $\beta$ 16 are monomeric in PBS. The spectrum of the SL-A $\beta$ 40 peptide under aggregation conditions has multiple components and broadened lines (figure 4.2) [20]. In figure 4.2, the spectra of the spin-labeled shorter peptides, SL-A $\beta$ 15 and SL-A $\beta$ 16, in PBS, are compared to that of the SL-A $\beta$ 40 peptide at the same peptide concentration. The differences of aggregation in SL-A $\beta$ 40 (broad lines, extra signals) are absent in the spectra of shorter peptides further emphasizing the absence of aggregation in SL-A $\beta$ 15 and SL-A $\beta$ 16.

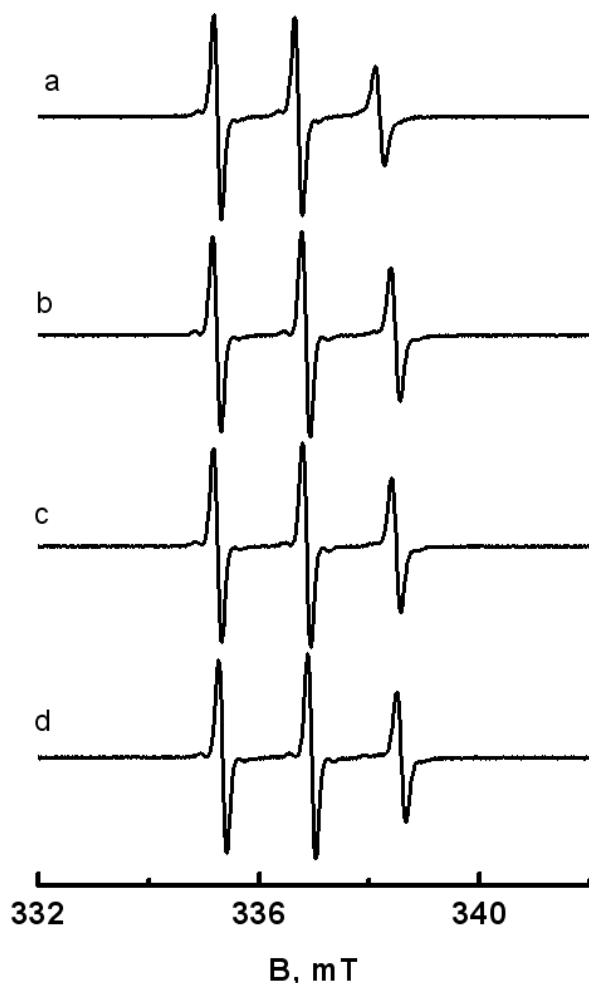


**Figure 4.1** Room temperature EPR spectra of SL-A $\beta$ 15 under different conditions. a: SL-A $\beta$ 15 in DMSO. b: Mixture of the diamagnetically diluted SL-A $\beta$ 15 (diamagnetically diluted SL-A $\beta$ 15 (dd-SL-A $\beta$ 15): a mixture of 86 % wild type A $\beta$ 15 and 14 % SL-A $\beta$ 15) with wild type A $\beta$ 15 in PBS (dd-SL-A $\beta$ 15: wild type A $\beta$ 15, 1:1). Total peptide concentration is 1.1 mM. c: Mixture of dd-SL-A $\beta$ 15 with wild type A $\beta$ 40 in PBS (dd-SL-A $\beta$ 15: wild type A $\beta$ 40, 1:1). Total peptide concentration is 1.1 mM. d: Mixture of dd-SL-A $\beta$ 15 with wild type A $\beta$ 40 in PBS (dd-SL-A $\beta$ 15: wild type A $\beta$ 40, 1:2). Total peptide concentration is 1.65 mM.

The EPR spectra of the shorter peptides in the presence of A $\beta$ 40 are similar to the spectra of the shorter peptides alone. Furthermore, the spectral line-shape of the shorter peptides did not change for the two concentrations of the A $\beta$ 40 peptide used (0.55 mM and 1.1 mM), showing the absence of interaction of A $\beta$ 15 and A $\beta$ 16 with A $\beta$ 40 (figure 4.1). These observations are confirmed by the similarity of the simulation parameters given in table 4.2.



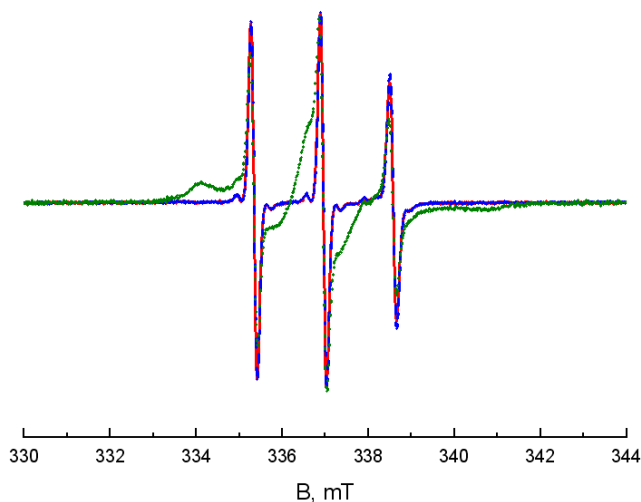


**Figure 4.2** Room temperature EPR spectra of SL-A $\beta$ 15, SL-A $\beta$ 16, and SL-A $\beta$ 40 under conditions, where A $\beta$ 40 aggregates. Red line: diamagnetically diluted SL-A $\beta$ 15, i.e., SL-A $\beta$ 15: wild type A $\beta$ 15 (14 % SL-A $\beta$ 15: 86 % wild type A $\beta$ 15). Blue line: diamagnetically diluted SL-A $\beta$ 16, i.e., SL-A $\beta$ 16: wild type A $\beta$ 16 (14 % SL-A $\beta$ 16: 86 % wild type A $\beta$ 16). Green line: diamagnetically diluted SL-A $\beta$ 40, i.e., SL-A $\beta$ 40: wild type A $\beta$ 40 (14 % SL-A $\beta$ 40: 86 % wild type A $\beta$ 40). Total peptide concentration is 0.55 mM for all samples.

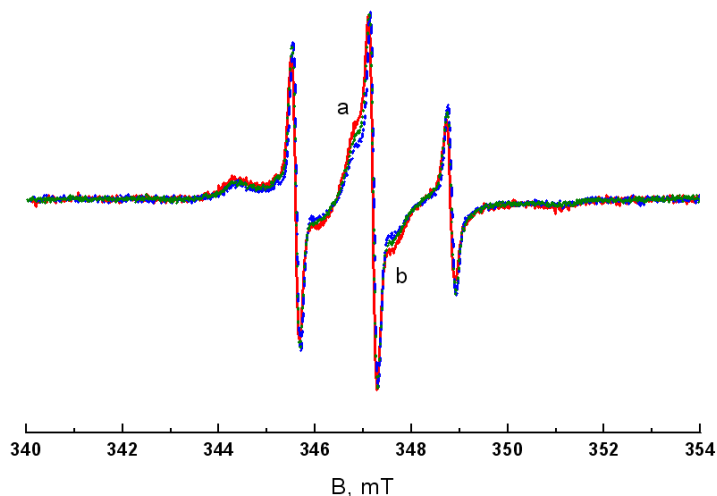


**Figure 4.3** Room temperature EPR spectra showing the effect of A $\beta$ 15 and A $\beta$ 16 on A $\beta$ 40. Red line: dd-SL-A $\beta$ 15 (14 % SL-A $\beta$ 15: 86 % wild type A $\beta$ 15): wild type A $\beta$ 40 (1:1). Blue line: dd-SL-A $\beta$ 16 (14 % SL-A $\beta$ 16: 86 % wild type A $\beta$ 16): wild type A $\beta$ 40 (1:1). Green line: dd-SL-A $\beta$ 40 (14 % SL-A $\beta$ 40: 86 % wild type A $\beta$ 40): wild type A $\beta$ 40 (1:1). Total peptide concentration is 1.1 mM for all samples. There is a small difference among the three spectra in regions a and b.

**Table 4.2** EPR parameters obtained from simulation for the SL-A $\beta$ 15 peptide and the SL-A $\beta$ 16 peptide in PBS and in DMSO. Given are:  $\tau_r$ , rotation-correlation time,  $A_{zz}$  is the hyperfine splitting along the z-direction, lw is the component line-width of the simulation.

sample	solvent	[total peptide] (mM)	$\tau_r$ (ns)	$A_{zz}$ (MHz)	lw (mT)
SL-A $\beta$ 15	DMSO	0.55	$0.17 \pm 0.02$	100	0.09
SL-A $\beta$ 15 + A $\beta$ 15	PBS	0.55	$0.10 \pm 0.02$	110	0.11
SL-A $\beta$ 15 + A $\beta$ 40	PBS	0.55	$0.11 \pm 0.02$	110	0.10
SL-A $\beta$ 15 + A $\beta$ 40	PBS	1.10	$0.15 \pm 0.02$	110	0.10
SL-A $\beta$ 16	DMSO	0.55	$0.18 \pm 0.02$	100	0.09
SL-A $\beta$ 16 + A $\beta$ 16	PBS	0.55	$0.10 \pm 0.02$	110	0.11
SL-A $\beta$ 16 + A $\beta$ 40	PBS	0.55	$0.11 \pm 0.02$	110	0.10
SL-A $\beta$ 16 + A $\beta$ 40	PBS	1.10	$0.15 \pm 0.02$	110	0.10

The spectra of the SL-A $\beta$ 40 peptide alone and of the SL-A $\beta$ 40 peptide in the presence of the unlabeled shorter peptides are shown in figure 4.3. By means of simulation <sup>[20]</sup>, we determined the  $\tau_r$  values of each mobility component (see materials and methods) and their contribution to the total spectra (table 4.3). The  $\tau_r$  values of the SL-A $\beta$ 40 peptide in the presence or absence of shorter peptides as well as the amount of each mobility component are given in table 4.3. There is a small difference among the three spectra in regions “a” and “b”, also reflected in small differences of the  $\tau_r$  values and their relative contributions (figure 4.3).

**Table 4.3** EPR parameters obtained from simulation for the A $\beta$ 40 peptide alone as well as in the presence of shorter peptides: A $\beta$ 15 and A $\beta$ 16. Given are:  $\tau_r$ , rotation-correlation time,  $A_{zz}$  is the hyperfine splitting along the z-direction, lw is the component line-width of the simulation and % stands for the contribution of the component to the total spectrum.

sample	fast				medium				slow			
	$\tau_r$ (ns)	$A_{zz}$ (MHz)	lw (mT)	%	$\tau_r$ (ns)	$A_{zz}$ (MHz)	lw (mT)	%	$\tau_r$ (ns)	$A_{zz}$ (MHz)	lw (mT)	%
SL-A $\beta$ 40	$0.19 \pm 0.04$	110	0.14	$12 \pm 2$	$2.50 \pm 0.35$	110	0.32	$52 \pm 2$	> 50	94	0.50	$36 \pm 2$
SL-A $\beta$ 40 + A $\beta$ 15	$0.19 \pm 0.04$	110	0.14	$11 \pm 2$	$2.50 \pm 0.35$	110	0.32	$53 \pm 2$	> 50	94	0.50	$36 \pm 2$
SL-A $\beta$ 40 + A $\beta$ 16	$0.19 \pm 0.04$	110	0.14	$15 \pm 2$	$2.50 \pm 0.35$	110	0.32	$47 \pm 2$	> 50	94	0.50	$37 \pm 2$

To determine whether these differences are significant with respect to the sample-to-sample variation we analyzed the ratios of the intensities of the fast to the slow component in each spectrum (figure 4.4) for a large set of samples. Although there is a difference in the intensity ratios of the fast to the slow component of the samples of the SL-A $\beta$ 40 peptide alone and those containing SL-A $\beta$  and the shorter

peptides, the differences are not significant, in view of the sample-to-sample variation.

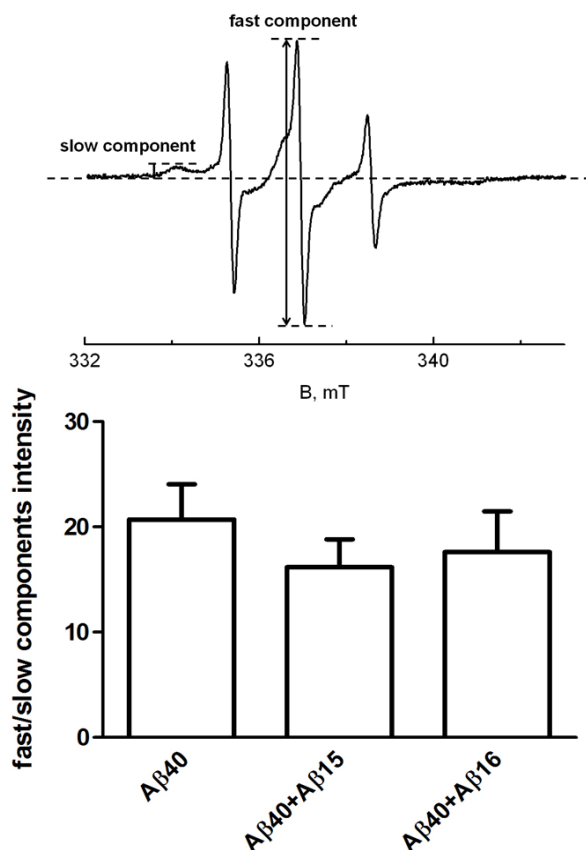


**Figure 4.4** Effect of short A $\beta$  peptides (A $\beta$ 15 and A $\beta$ 16) on the aggregation of A $\beta$ 40. Intensity ratios of the fast/slow components of three A $\beta$  samples; A $\beta$ 40, A $\beta$ 40 + A $\beta$ 15 and A $\beta$ 40 + A $\beta$ 16 are represented as mean  $\pm$  SEM of three sets of samples, i.e., each A $\beta$  sample was fibrillized and measured under the same conditions three times.

An increase in fluorescence of the fibril-specific dye ThioT, compared to the fluorescence of the free ThioT in PBS buffer, is a marker for fibril formation. Relative fluorescence levels for the samples are shown in figure 4.5. The fluorescence level increased in the samples with the full-length peptide, while no fluorescence increase is observed in the samples which contained only the shorter peptides. Samples containing an equivalent amount of shorter peptides and the full-length A $\beta$  (0.55 mM: 0.55 mM), have a fluorescence level similar to that of pure 0.55 mM full-length A $\beta$  samples, whereas the fluorescence in a sample with 1.1

mM full-length A $\beta$  is significantly higher compared to that of 0.55 mM full-length A $\beta$ .

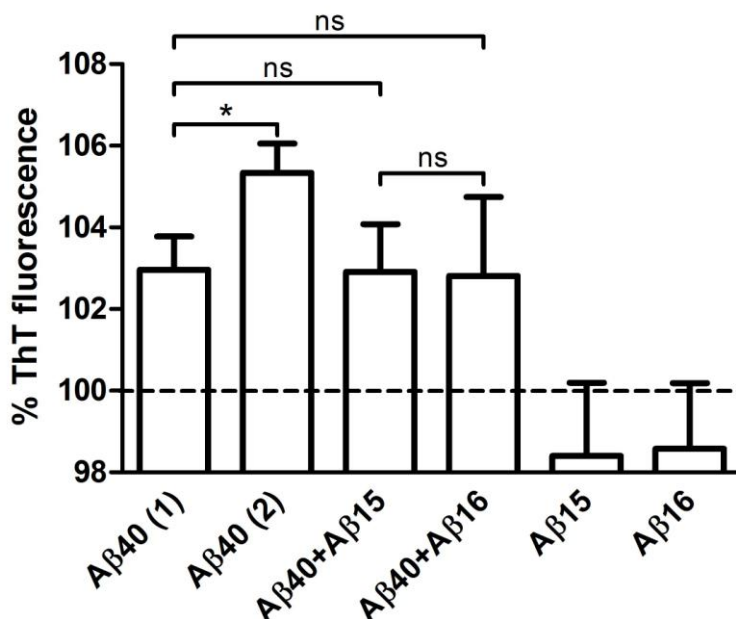


**Figure 4.5** ThioT fluorescence (%) of six A $\beta$  samples; A $\beta$ 40 (1) (0.55 mM), A $\beta$ 40 (2) (1.1 mM), A $\beta$ 40 + A $\beta$ 15 (0.55 mM), A $\beta$ 40 + A $\beta$ 16 (0.55 mM), A $\beta$ 15 (0.55 mM), A $\beta$ 16 (0.55 mM). For ThioT readings the peptide was diluted to concentrations of 11 or 27.5  $\mu$ M. Values for ThioT fluorescence of ThioT alone were set to 100 % and the ThioT fluorescence of all samples is reported relative to this value (mean  $\pm$  SEM of three experiments, i.e., each A $\beta$  sample was fibrillized and measured under the same conditions three times; \* $p$  < 0.05 unpaired t test, ns: not significant).

#### 4.4 Discussion

The aim of this study was to investigate and compare the aggregation potential of the two shorter N-terminal A $\beta$  peptides A $\beta$ 15 and A $\beta$ 16 and to determine if the shorter peptides had an effect on the aggregation of the A $\beta$ 40 peptide. To monitor the aggregation we used spin-label EPR by which, previously, the aggregation of the A $\beta$ 40 peptide was studied<sup>[20,34]</sup>. In the present study either the short peptides (SL-A $\beta$ 15 or SL-A $\beta$ 16) or the A $\beta$ 40 (SL-A $\beta$ 40) peptide was spin labeled. By measuring the spin-label mobility of the SL-A $\beta$ 15 and the SL-A $\beta$ 16 in the absence/presence of the wild type A $\beta$ 40 or measuring the spin-label mobility of SL-A $\beta$ 40 in the presence of either wild type short peptides, the properties of each of the components of the aggregating samples was monitored individually.

For the short A $\beta$  fragments, A $\beta$ 15 and A $\beta$ 16, the ThioT results show the absence of fibril formation. The same is true for the EPR results, where an observed trend towards larger  $\tau_r$  values at higher concentrations of A $\beta$  (given in table 4.2 and results) most likely is not a sign of aggregation, but an effect of the increasing viscosity of the solution.

The behavior of A $\beta$ 15 and A $\beta$ 16 is not affected by the presence of A $\beta$ 40, which reveals that the full-length A $\beta$  does not induce aggregation in A $\beta$ 15 or A $\beta$ 16. Furthermore, no evidence for interaction of A $\beta$ 15 or A $\beta$ 16 with A $\beta$ 40 is observed. The A $\beta$ 40, on the other hand does aggregate under these conditions as is demonstrated in the experiments where SL-A $\beta$ 40 was monitored in the presence of unlabeled A $\beta$ 15 and A $\beta$ 16. In these experiments the difference between the EPR spectra is not significant (figure 4.3), revealing that the shorter peptides also do not inhibit or promote aggregation of full-length A $\beta$  (table 4.3).

Previous reports about the aggregation of A $\beta$ 15 and A $\beta$ 16 had differing outcomes. As in the present study, NMR investigations at high concentrations of A $\beta$ 16 showed the absence of aggregation <sup>[17-19]</sup>. Similarly, Liu <sup>[14]</sup> and Liao <sup>[15]</sup> conclude from CD, AFM, and ThioT that A $\beta$ 16 does not aggregate. In contrast, a recent study <sup>[16]</sup> proposes that A $\beta$ 16 can assemble into a novel type of toxic oligomers and fibrils. These findings cannot be reconciled with the present study unless only a small fraction of the peptide (< 10 %) was in the oligomeric state in the AFM samples.

In summary, we find that the short peptides A $\beta$ 15 or A $\beta$ 16 do not directly influence the aggregation of A $\beta$ 40. This reveals that the effects that these short peptides show in neurotoxicity essays cannot derive from a direct influence of A $\beta$ 15 and A $\beta$ 16 on the aggregation of full-length A $\beta$ . An alternative pathway for their action could be related to the metal-binding site in the N-terminus of A $\beta$  <sup>[27,35-49]</sup>. The fragments A $\beta$ 15 and A $\beta$ 16 contain all ligands that were proposed for binding Cu (II) and Zn (II) ions that were suggested to increase A $\beta$  aggregation. The short fragments could reduce A $\beta$  aggregation, because they scavenge the metal ions making the full-length A $\beta$  less prone to aggregation.

Overall, the present EPR investigation suggests that the short peptides A $\beta$ 15 or A $\beta$ 16 do not influence the aggregation of A $\beta$ 40 directly, supporting the view that physiological effects of these shorter fragments occur via a different route, possibly via metal-ion interactions. Therefore, examining the effect of metal ions on the aggregation of A $\beta$ 40 in the presence of the short peptides A $\beta$ 15 or A $\beta$ 16 is suggested as a future line of investigation.

## Reference List

- [1] K. Chopra, S. Misra, A. Kuhad, *Expert.Opin.Ther.Targets*. **2011**, 15 535-555.
- [2] R. Jakob-Roetne, H. Jacobsen, *Angew.Chem.Int.Ed Engl*. **2009**, 48 3030-3059.
- [3] F. Panza, V. Solfrizzi, V. Frisardi, C. Capurso, A. D'Introno, A. M. Colacicco, G. Vendemiale, A. Capurso, B. P. Imbimbo, *Drugs Aging* **2009**, 26 537-555.
- [4] D. J. Selkoe, *Ann.Intern.Med*. **2004**, 140 627-638.
- [5] D. J. Selkoe, *Neuron* **1991**, 6 487-498.
- [6] E. Portelius, G. Brinkmalm, A. Tran, U. Andreasson, H. Zetterberg, A. Westman-Brinkmalm, K. Blennow, A. Ohrfelt, *Exp.Neurol*. **2010**, 223 351-358.
- [7] E. Portelius, N. Mattsson, U. Andreasson, K. Blennow, H. Zetterberg, *Curr.Pharm.Des* **2011**, 17 2594-2602.
- [8] A. Awasthi, Y. Matsunaga, T. Yamada, *Exp.Neurol*. **2005**, 196 282-289.
- [9] E. Portelius, H. Zetterberg, U. Andreasson, G. Brinkmalm, N. Andreassen, A. Wallin, A. Westman-Brinkmalm, K. Blennow, *Neurosci.Lett*. **2006**, 409 215-219.
- [10] C. Soto, G. P. Saborio, B. Permanne, *Acta Neurol.Scand.Suppl* **2000**, 176 90-95.
- [11] Y. Matsunaga, A. Fujii, A. Awasthi, J. Yokotani, T. Takakura, T. Yamada, *Regul.Pept*. **2004**, 120 227-236.
- [12] J. F. Leverone, E. T. Spooner, H. K. Lehman, J. D. Clements, C. A. Lemere, *Vaccine* **2003**, 21 2197-2206.
- [13] H. Li, J. Zou, Z. Yao, J. Yu, H. Wang, J. Xu, *J.Neuroimmunol*. **2010**, 219 8-16.
- [14] R. Liu, C. McAllister, Y. Lyubchenko, M. R. Sierks, *J.Neurosci.Res*. **2004**, 75 162-171.
- [15] M. Q. Liao, Y. J. Tzeng, L. Y. Chang, H. B. Huang, T. H. Lin, C. L. Chyan, Y. C. Chen, *FEBS Lett*. **2007**, 581 1161-1165.
- [16] X. T. Du, L. Wang, Y. J. Wang, M. Andreasen, D. W. Zhan, Y. Feng, M. Li, M. Zhao, D. Otzen, D. Xue, Y. Yang, R. T. Liu, *J.Alzheimers Dis*. **2011**, 27 401-413.
- [17] A. N. Istrate, P. O. Tsvetkov, A. B. Mantsyzov, A. A. Kulikova, S. A. Kozin, A. A. Makarov, V. I. Polshakov, *Biophys.J*. **2012**, 102 136-143.
- [18] P. O. Tsvetkov, A. A. Kulikova, A. V. Golovin, Y. V. Tkachev, A. I. Archakov, S. A. Kozin, A. A. Makarov, *Biophys.J*. **2010**, 99 L84-L86.
- [19] S. Zirah, S. A. Kozin, A. K. Mazur, A. Blond, M. Cheminant, I. Segalas-Milazzo, P. Debey, S. Rebuffat, *J.Biol.Chem*. **2006**, 281 2151-2161.
- [20] I. Sepkhanova, M. Drescher, N. J. Meeuwenoord, R. W. A. L. Limpens, R. I. Koning, D. V. Filippov, M. Huber, *Applied Magnetic Resonance* **2009**, 36 209-222.
- [21] M. Margittai, R. Langen, *Q.Rev.Biophys*. **2008**, 41 265-297.
- [22] F. Scarpelli, M. Drescher, T. Rutters-Meijneke, A. Holt, D. T. Rijkers, J. A. Killian, M. Huber, *J.Phys.Chem.B* **2009**, 113 12257-12264.
- [23] D. C. Rambaldi, A. Zattoni, P. Reschiglian, R. Colombo, L. E. De, *Anal.Bioanal.Chem*. **2009**, 394 2145-2149.
- [24] A. L. Cloe, J. P. Orgel, J. R. Sachleben, R. Tycko, S. C. Meredith, *Biochemistry* **2011**, 50 2026-2039.
- [25] S. Stoll, A. Schweiger, *Journal of Magnetic Resonance* **2006**, 178 42-55.
- [26] S. Steigmliller, M. Börsch, P. Gräber, M. Huber, *Biochim.Biophys.Acta* **2005**, 1708 143-153.
- [27] Q. F. Ma, J. Hu, W. H. Wu, H. D. Liu, J. T. Du, Y. Fu, Y. W. Wu, P. Lei, Y. F. Zhao, Y. M. Li, *Biopolymers* **2006**, 83 20-31.
- [28] M. N. Oda, T. M. Forte, R. O. Ryan, J. C. Voss, *Nat.Struct.Biol*. **2003**, 10 455-460.
- [29] H. LeVine, III, *Protein Sci*. **1993**, 2 404-410.
- [30] H. Naiki, K. Higuchi, M. Hosokawa, T. Takeda, *Analytical Biochemistry* **1989**, 177 244-249.
- [31] K. Broersen, F. Rousseau, J. Schymkowitz, *Alzheimers Res.Ther*. **2010**, 2 12.
- [32] K. Broersen, W. Jonckheere, J. Rozenski, A. Vandersteen, K. Pauwels, A. Pastore, F. Rousseau, J. Schymkowitz, *Protein Eng Des Sel* **2011**, 24 743-750.
- [33] M. L. Giuffrida, F. Caraci, B. Pignataro, S. Cataldo, B. P. De, V. Bruno, G. Molinaro, G. Pappalardo, A. Messina, A. Palmigiano, D. Garozzo, F. Nicoletti, E. Rizzarelli, A. Copani, *J.Neurosci*. **2009**, 29 10582-10587.

- [34] A. Paivio, J. Jarvet, A. Gräslund, L. Lannfelt, A. Westlind-Danielsson, *Journal of Molecular Biology* **2004**, 339 145-159.
- [35] O. N. Antzutkin, *Magnetic Resonance in Chemistry* **2004**, 42 231-246.
- [36] C. S. Atwood, R. C. Scarpa, X. Huang, R. D. Moir, W. D. Jones, D. P. Fairlie, R. E. Tanzi, A. I. Bush, *J.Neurochem.* **2000**, 75 1219-1233.
- [37] C. C. Curtain, F. Ali, I. Volitakis, R. A. Cherny, R. S. Norton, K. Beyreuther, C. J. Barrow, C. L. Masters, A. I. Bush, K. J. Barnham, *J.Biol.Chem.* **2001**, 276 20466-20473.
- [38] P. Dorlet, S. Gambarelli, P. Faller, C. Hureau, *Angew.Chem.Int.Ed Engl.* **2009**, 48 9273-9276.
- [39] J. A. Duce, A. Tsatsanis, M. A. Cater, S. A. James, E. Robb, K. Wikke, S. L. Leong, K. Perez, T. Johanssen, M. A. Greenough, H. H. Cho, D. Galatis, R. D. Moir, C. L. Masters, C. McLean, R. E. Tanzi, R. Cappai, K. J. Barnham, G. D. Ciccotosto, J. T. Rogers, A. I. Bush, *Cell* **2010**, 142 857-867.
- [40] E. House, J. Collingwood, A. Khan, O. Korchazkina, G. Berthon, C. Exley, *J.Alzheimers.Dis.* **2004**, 6 291-301.
- [41] X. Huang, C. S. Atwood, R. D. Moir, M. A. Hartshorn, R. E. Tanzi, A. I. Bush, *J.Biol.Inorg.Chem.* **2004**, 9 954-960.
- [42] D. Jiang, X. Li, L. Liu, G. B. Yagnik, F. Zhou, *J.Phys.Chem.B* **2010**, 114 4896-4903.
- [43] T. Kowalik-Jankowska, M. Ruta, K. Wisniewska, L. Lankiewicz, *J.Inorg.Biochem.* **2003**, 95 270-282.
- [44] T. Kowalik-Jankowska, M. Ruta, K. Wisniewska, L. Lankiewicz, M. Dyba, *J.Inorg.Biochem.* **2004**, 98 940-950.
- [45] S. A. Kozin, Y. V. Mezentsev, A. A. Kulikova, M. I. Indeykina, A. V. Golovin, A. S. Ivanov, P. O. Tsvetkov, A. A. Makarov, *Mol.Biosyst.* **2011**, 7 1053-1055.
- [46] B. K. Shin, S. Saxena, *Biochemistry* **2008**, 47 9117-9123.
- [47] C. D. Syme, R. C. Nadal, S. E. J. Rigby, J. H. Viles, *Journal of Biological Chemistry* **2004**, 279 18169-18177.
- [48] P. O. Tsvetkov, I. A. Popov, E. N. Nikolaev, A. I. Archakov, A. A. Makarov, S. A. Kozin, *Chembiochem* **2008**, 9 1564-1567.
- [49] H. Yu, J. Ren, X. Qu, *Chembiochem* **2008**, 9 879-882.

